Final Report for DOE FG02-99ER62797

Specific Aims

The overall goal of this proposal has been to develop and interface a new technology, molecular gates, with microfabricated systems to add an important capability to microfabricated DNA measurement systems. This project specifically focused on demonstrating how molecular gates could be used to capture a single analyte band, among a stream of bands from a separation or a flow injection analysis experiment, and release it for later measurement, thus allowing further manipulations on the selected analyte. Since the original proposal, the molecular gate concept has been greatly expanded to allow the gates to be used as externally controllable intelligent interconnects in multilayer microfluidic networks. We have demonstrated: (1) the ability of the molecular gates to work with a much wider range of biological molecules including DNA, proteins and small metabolites; and (2) the capability of performing an electrophoretic separation and sequestering individual picoliter volume components (or even classes of components) into separate channels for further analysis. Both capabilities will enable characterization of small mass amounts of complex mixtures of DNA, proteins and even small molecules – allowing them to be further separated and chemically characterized.

Significance

Analyzing the chemical diversity of an organism is a grand challenge problem which inherently requires the development of sophisticated analytical methods – broadly construed the ability to separate components of interest at levels down to and below the level of single cells and to identify and characterize these components. In modern DNA sequencers, for example, sample handling, separation and detection are highly automated, and are based on high efficiency capillary electrophoresis separations and sensitive laser induced fluorescence detection.

Can the degree of automation and versatility offered by modern genome instrumentation be brought to the analytical methods relevant to proteomics and metabolomics (small molecule characterization)? The analysis of these classes of molecules offers a much more complex set of problems than those posed by DNA. For example there are a large number of options in mass analyzers, and other characterization choices. Often these require much larger amounts of samples than required for DNA, necessitated by the sample handling needed to separate and introduce the samples in the correct chemical environment for each type of instrumentation. For example, most proteomics efforts are centered around either MALDI or ESI mass spectrometry, each of which places severe constraints on the separation conditions that can be used. Small molecule assays greatly depend on the molecular type. How can these separate steps be truly independent from each other? What is desperately needed is the ability to segregate a sample into molecular subtypes, and subsequently separate these into molecular fractions, so the chemical environment can be manipulated before detection. This critically important area

– molecular manipulations, transport and capture for proteins and metabolic products – was the target of our research.

Results of DOE FG02-99ER62797 Funded Research

New ways to control the movement of fluids at the micrometer scale enable the application of microfluidic devices to molecular separations and other forefront technologies[1-10], but currently only analytical separations are accessible to microfluidics, primarily because the two-dimensional nature of current microfluidics makes complex band manipulations cumbersome. Extension of microfluidic devices to three-dimensions would open new vistas and specifically would enable preparative microfluidic separations. For example, gated transfer could be used to collect attomole-level bands separated by chip-based electrophoresis and hold them for further processing or characterization, thereby creating preparative forms of chromatography operating at heretofore-unattainable low sample levels. Furthermore, such multi-level microfluidic structures parallel the massively three-dimensional architectures characteristic of electronic devices and open the way for complex fluidic manipulations. However, the creation of true multi-level fluidic devices has proven to be a challenging task. Early examples of three-dimensional microfluidic flow used discrete microchannels to bridge, rather than connect, independent analysis modules for the realization of a micro-total analysis system[11, 12], and to alleviate space constraints[13]. These topologically complex systems led to microvalves and micromixers[14, 15] and even pressure-actuated valves[16].

We have developed a critical extension of fluidic circuitry to exploit the third dimension, namely a nanofluidic gateable (externally controllable) interconnect between microfluidic layers. Nanoporous membranes containing 15- to 200-nm wide cylindrical pores are employed as interconnects to establish controllable fluidic communication between micron-scale channels operating in vertically separated planes (Fig. 1). Fluidic communication can be

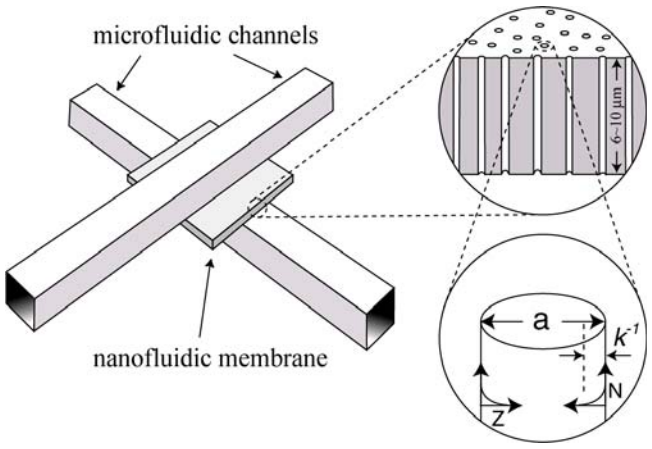

Fig 1. Upper left: Schematic diagram of the crossed microfluidic channels separated by a nanofluidic membrane (light gray at intersection). *Upper right*: The cross-sectional schematic of the nanoporous membrane illustrates the large aspect ratios characteristic of the nanopores employed. Typical length-to-width ratios were in the range 20 – 350 for membranes used in this work. *Lower right*: Schematic diagram showing relative sizes of the channel diameter (*a*) and Debye length typically encountered with nanometer diameter channels and millimolar electrolyte solutions. Z is the distance from the nanochannel wall, and N is the ion number density.

established among any number of vertically stacked planes with the nanoporous membranes acting as a non-moving valve between the layers. These interconnects provide controllable transport of components at the desired point in space and time between the functional layers of a complex device.

The crossed microfluidic channels shown in Fig. 1 spatially define the transport region and eliminate the need for precise alignment of the nanofluidic membrane. Analyte transport is interrogated by monitoring the fluorescence signal on either the source or the receiving channel side of the nanofluidic membrane. Fig. 2a shows the transfer of the anionic fluorophore, fluorescein, across a 200-nm pore diameter nuclear track-etched polycarbonate (PCTE) membrane to a buffer-filled receiving channel held at ground potential in the off-state. Successive transfers are effected by application of negative bias pulses. The fluorophore concentration probed during bias application is a balance between active transport from the source channel and diffusion along the receiving channel. When the bias is removed, diffusion depletes the concentration in the region probed, but with successive forward bias applications the concentration of probe in the receiving channel increases, thereby diminishing the driving force for diffusion after subsequent transfers. In a similar experiment, directional flow is maintained in the receiving channel (Fig 2b). The build-up to steady-state at the membrane after bias application, clearly more gradual than that without flow, results from the balance between active transport of the analyte across the nanofluidic membrane and its removal by cross-flow in the receiving channel. An obvious time offset is observed when the detection region is moved downstream of the interconnect (Fig. 2b). Fig. 2c demonstrates the level of control and speed of transfer possible with these nanofluidic interconnects. In this experiment the off-state voltages are allowed to float, producing a non-zero level of transfer intermediate between the forward-bias (-60 V) on-state and the reverse-bias (+ 60 V) on-state. Measurements on the changing edges of Fig. 2c indicate steady state concentration is re-established in the receiving channel within ~ 1.2 s of applying the switching voltage. Fig. 2d demonstrates the insensitivity to analyte charge state by comparing the transfer of the neutral fluorophore bodipy.

By choosing the pore diameter, pore surface chemistry, channel surface charge, and solution composition, one can select the direction that fluid flows through the pore for the same externally applied voltage. Interestingly, this flow is directly opposite to the direction based on the electroosmotic flow characteristics of the 200-nm pore diameter PCTE membrane alone[17]. The surfaces of the PCTE membrane channels are coated with polyvinylpyrrolidone (PVP) to render them hydrophilic. The tertiary amine of the PVP is susceptible to protonation, making the surface net positive at pH 8, thus recruiting a population of negative solution counterions to the interior of the nanochannels. Under the low ionic strength conditions used here, the ionic population in the channel is predominantly $H_2PO_4^-/HPO_4^{2-}$, so forward bias is obtained with $V_{rec} - V_{source} > 0$, if the nanofluidic channels control the direction of transport. Instead, flow in the direction predicated on the (negative) charge state of the poly(dimethylsiloxane), PDMS, surfaces of the microfluidic channels controls transport. Figs. 3a and 3b demonstrate that the direction of flow is reversed for transport across a 200-nm pore diameter membrane compared with that across a 15-nm pore diameter membrane. This behavior can be understood based on two effects – the greatly increased resistance to pressure driven flow

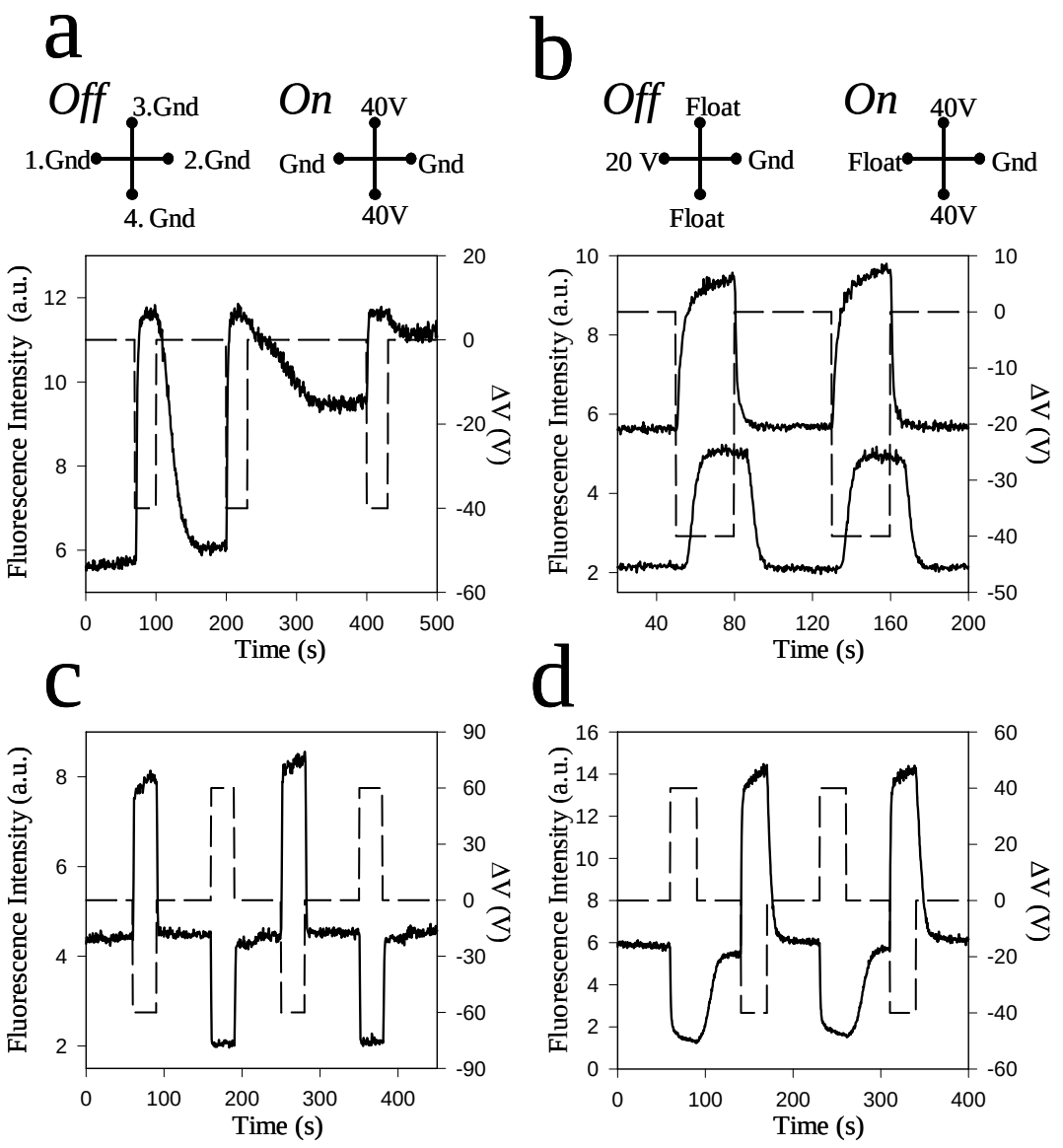

Fig 2. Fluorescence intensity (left ordinate, solid line) and applied bias, Δ*V*, (right ordinate, dashed line) as a function of time showing transport of 170 nM fluorescein across a 200-nm pore diameter PCTE membrane. The inset shows how the bias voltages were applied. Contacts 1 and 2 are in the receiving (horizontal) channel; contacts 3 and 4 are in the source (vertical) channel. The receiving channel was held under flow-free conditions during the off-state in this experiment. (b) Fluorescence intensity and applied bias as a function of time to monitor the transport of 0.17 μM fluorescein across a 200-nm pore diameter PCTE detected at (*left*) the membrane and 100 μm downstream (*right*) in the receiving channel. On and off bias potentials (inset) were designed to produce flow in the receiving channel. (c) Fluorescence intensity and applied bias as a function of time across 200-nm pore diameter PCTE. Off-state, reverse bias, and forward bias potentials are shown in the inset. (d) Neutral probe migration. Fluorescence intensity and applied bias as a function of time to monitor the transport of 900 nM bodipy fluorophore across 200-nm pore diameter PCTE membrane.

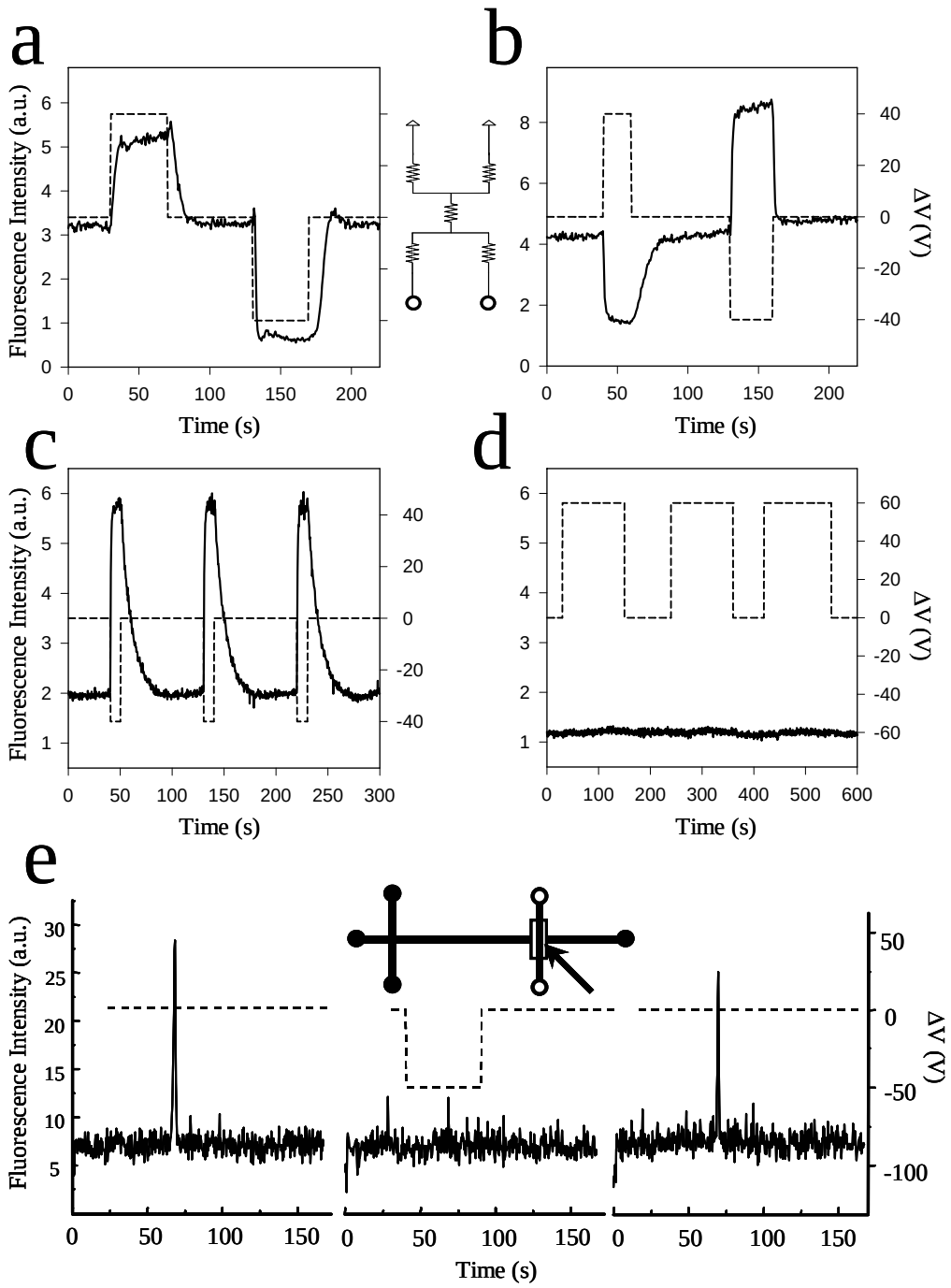

Fig. 3. The migration of a probe across PCTE membranes with (a) 15-nm and (b) 200-nm (*right*) pore diameters connecting two 100-μm wide PDMS channels. Fluorescence intensity and applied bias ΔV as a function of time to monitor the transport of 170 nM fluorescein. The inset shows an impedance network model for the combined microfluidic and nanofluidic channels. Electrokinetic macromolecular transport of 2 MDa FITC-labeled dextrans (40 nM) across (c) 200-nm and (d) 15-nm pore diameter PCTE membranes. (e) Three successive injections of 200 nM fluorescein in 10 mM sodium dodcelysulfonate and 10 mM Tris-borate buffer in a capillary electrophoresis microchip monitored just after the membrane gate (inset shows the sampling geometry). The gate sampling voltage (dashed line, right ordinate) is shown in each panel. Sampling was turned on only in the center panel.

integrate these individual components into multilayer structures with external control for the intelligent transfer of individually selectable analytes between layers, will enable many heretofore unattainable applications.

During this project, the molecular gate concept evolved from the initial concept of a multilayer membrane that can collect and release analytes from the effluent of a separation capillary into an integrated structure of great power and versatility. Not only can molecular gates act as a no-moving parts valve between multilayer microfabricated devices, but they can impart selectivity, such as demonstrated in the size-based transfer above. We have demonstrated the ability to separate and manipulate DNA, amino acids and large dextrans.

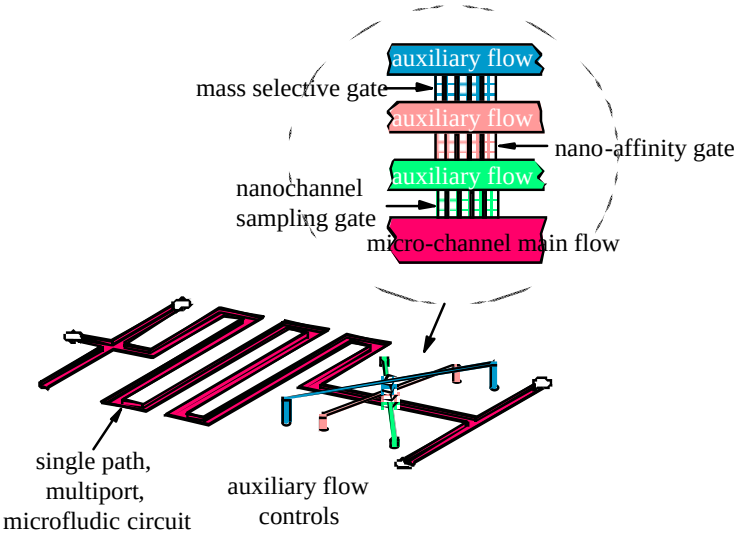

Fig. 4. Capillary electrophoresis on a chip with vertically integrated nanomembrane stack for integral sampling. A single parallel stack of nanoporous membranes is used to illustrate the concept of a multilayer device with selection based on different molecular characteristics, *e.g.*, electrophoretic mobility, affinity, and size.

The basic unit operations we have demonstrated point to an exciting future. By incorporating multiple channels into our hybrid molecular gate separation device, parallel gate arrays can be fabricated and applied to complex molecular manipulations. The ultimate extension of this concept using parallel channels – by repetitive splitting of channels in-the-plane and equipping each channel with several molecular gates (see Figure 5) – will enable a set of parallel analytical measurements to be performed which simply is beyond the reach of the current measurement paradigm.

In the simplest manifestation of this concept a second channel can be added so that the gates both inject a sample and collect the analyte. With many channels, we can collect a suite of analytes into individual channels. In the preliminary experiment shown in Fig. 6, we used two parallel channels, p_1 and p_2, 425 μm apart, intersecting a cross-channel, c. From such a preliminary device, Fig. 6c-6g shows a sequence of fluorescence images from injection to collection. Our model compound, fluorescein, is electrokinetically injected from

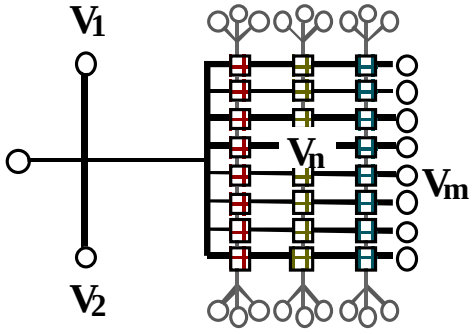

Fig. 5. A multiple-path, multiport, microfluidic circuit with a distributed array of interconnects that can be used to capture and select specific analyte bands.

p_1 into the cross channel, Fig. 6d. Subsequently, the electrical configuration is switched to move the fluorescein band along the cross channel, Fig. 6e. Knowing the velocity in the cross channel and the injection time allows timing the forward bias of the c-p_2 junction to move the band vertically into channel p_2, Fig. 6f. After reversing the bias, a slight broadening of the captured band is observed in p_2, Fig. 6g, attributed to diffusion. Selective transport of a single band out of multiple repeated injections is achieved in the same fashion, assuring the preparative manipulations envisioned above can be realized. The goal is to perform a separation and selectively capture select analytes into a second set of channels, move them enough to offset them from the first channel, move them back to the first layer for additional separation under differing conditions, and then selectively capture select band back to the upper layer.

In this way, a multistage separation can be performed under differing conditions on selected analytes, each of which would then be sequestered into its own channel. This approach could potentially revolutionize coupled separation-mass spectrometric detection experiments, because after separation analytes can be moved into a solution containing (or lacking) specific compounds that help or hinder MS detection. Perhaps even more exciting is the possibility of carrying out post-separation chemical reactions. For example, small molecules can easily be derivatized after a separation by using a collection channel seeded with the appropriate reagents. The power of this approach is apparent when one realizes that the typical nanometer distances between individual nanochannel openings in the plane of the membrane means that once the separated compound is transferred to the second channel diffusion is an effective means of mixing reagents, thus obviating the need for clumsy convective mixers to overcome the laminar flow profiles characteristic of microchannel electrokinetic transport. Thus, derivatization solutions can be optimized independently, and the assay of multiple classes of molecules requiring vastly differing solution chemistries can be achieved by transferring the molecules across a gate into a channel containing a different composition, pH, ionic strength *etc*. While an advantage of the multilayer approach is that the solution composition in the channels separated by molecular gates can be independently optimized, we have yet to fully explore this capability, nor understand the limits of such composition differences. Thus, such active feedback of sample band collection combined with potential additional separations will enable the optimization of a complex molecular fractionation on-the-fly to control any needed additional separation stages along with sample collection, all without the need for operator intervention. This truly promises to become an enabling technology in ultra-small sample manipulation and handling, and the research from DOE FG02-99ER62797 will be extended to a wide range of macromolecules using a series of custom fabricated devices.

Publications Resulting From Funding:

Nanocapillary Arrays Effect Mixing and Reaction in Multilayer Fluidic Structures, T.-C. Kuo, H.K. Kim, D.M. Cannon, Jr., M.A. Shannon, J.V. Sweedler, P.W. Bohn, **Angew. Chem, Int. Ed. Engl. 43**, 2004, 1862-1865.

Gateable Nanofluidic Interconnects for Multilayered Microfluidic Separation Systems, T.C. Kuo, D.M. Cannon, Jr, Y. Chen, J.J. Tulock, M.A. Shannon, J.V. Sweedler, P.W. Bohn, **Anal. Chem. 75**, 2003, 1861-7.

Nanocapillary Array Interconnects for Gated Analyte Injections and Electrophoretic Separations in Multilayer Microfluidic Architectures, D.M. Cannon, Jr., Kuo, T.C. Kuo, P.W. Bohn, J.V. Sweedler, **Anal. Chem. 75**, 2003, 2224-2230.

Manipulating Molecular Transport Through Nanoporous Membranes by Control of Electrokinetic Flow: Effect of Surface Charge Density and Debye Length. T.C. Kuo, L.A. Sloan, J.V. Sweedler, P.W. Bohn, **Langmuir 17**, 2001, 6298-6303.

Hybrid Three-Dimensional Nanofluidic/Microfluidic Devices Using Molecular Gates, T.-C. Kuo, D. Cannon Jr., M.A. Shannon, P.W. Bohn, J.V. Sweedler, **Sensors and Actuators A: Physical 102**, 2003, 223-233.

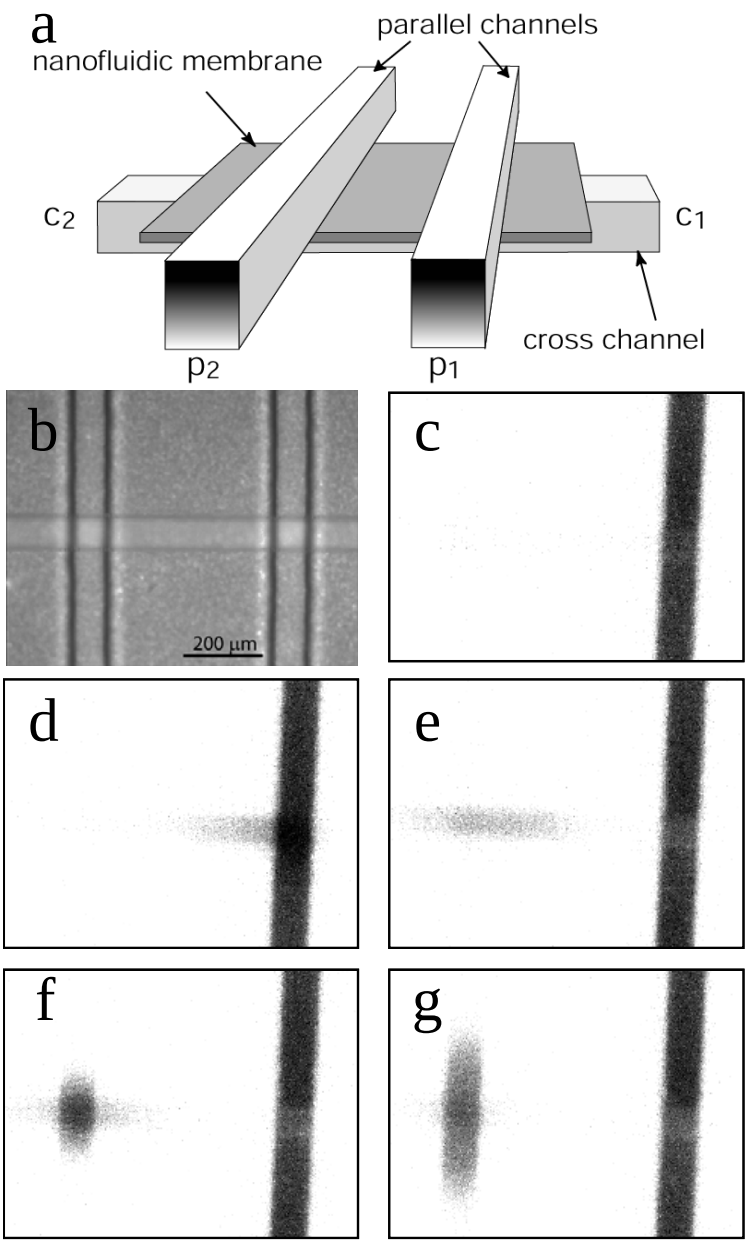

Fig 6. Injection and collection of an analyte band in a prototype device. (a) Schematic of the parallel-cross channel system (not to scale). The parallel channels p_1 and p_2 are embedded in the upper PDMS layer, separated by a 200-nm pore diameter PCTE membrane from a cross channel, c in the lower PDMS layer. (b) White light image of the interrogated area. (c) to (g) Fluorescence images of the injection/collection sequence. Channel p_1 was filled with 2 μM fluorescein^{2-} in 5 mM pH 9 PB, and the channels c and p_2 were filled with 5 mM pH 9 PB initially. (c) All reservoirs grounded. (d) Injection with 40 V bias across p1-c junction. (e) Moving the injected band in the cross channel with 40 V bias between c1 and c2. (f) Collection of the fluorescein band with 40 V bias applied to the c-p_2 junction. (g) Collection voltage off, but 40 V bias was applied between c1 and c2 to maintain flow.

Literature Cited

(1) Terry, S. C.; Jerman, J. H.; Angell, J. B. *IEEE Trans. Electron Devices* **1979**, *ED-26*, 1880-1886.

(2) Manz, A.; Graber, N.; Widmer, H. M. *Sens. Actuators, B* **1990**, *1*, 244-248.

(3) Harrison, D. J.; Fluri, K.; Seiler, K.; Fan, Z.; Effenhauser, C. S.; Manz, A. *Science (Washington, D.C.)* **1993**, *261*, 895-897.

(4) Jacobson, S. C.; Hergenroder, R.; Koutny, L. B.; Warmack, R. J.; Ramsey, J. M. *Anal. Chem.* **1994**, *66*, 1107-1113.

(5) Woolley, A. T.; Mathies, R. A. *Proc. Natl. Acad. Sci. U.S.A.* **1994**, *91*, 11348-11352.

(6) Haab, B. B.; Mathies, R. A. *Anal. Chem.* **1999**, *71*, 5137-5145.

(7) Koch, M.; Schabmueller, C. G. J.; Evans, A. G. R.; Brunnschweiler, A. *Sens. Actuators, A* **1999**, *74*, 207-210.

(8) Beebe, D. J.; Moore, J. S.; Bauer, J. M.; Yu, Q.; Liu, R. H.; Devadoss, C.; Jo, B. H. *Nature* **2000**, *404*, 588-590.

(9) McDonald, J. C.; Duffy, D. C.; Anderson, J. R.; Chiu, D. T.; Wu, H. K.; Schueller, O. J. A.; Whitesides, G. M. *Electrophoresis* **2000**, *21*, 27-40.

(10) Philpott, M. L.; Beebe, D. J.; Fischer, A.; Flachsbart, B.; Marshall, M.; Miller, N. R.; Selby, J. C.; Shannon, M. A.; Wu, Y., Hilton Head Island, SC, June 4 - 8 2000; 226-229.

(11) van der Schoot, B. H.; Jeanneret, S.; van den Berg, A.; de Rooij, N. F. *Sens. Actuators B* **1992**, *6*, 57-60.

(12) Fettinger, J. C.; Manz, A.; H., L.; Widmer, H. M. *Sens. Actuators B* **1993**, *17*, 19-25.

(13) Chiu, D. T.; Li Jeon, N.; Huang, S.; Kane, R. S.; Wargo, C. J.; Choi, I. S.; Ingber, D. E.; Whitesides, G. M. *Proc. Natl. Acad. Sci. U. S. A.* **2000**, *97*, 2408-2413.

(14) González, C.; Smith, R. L.; Howitt, D. G.; Collins, S. D. *Sens. Actuators A* **1998**, *66*, 315-322.

(15) Gray, B. L.; Jaeggi, D.; Mourlas, N. J.; van Drieenhuizen, B. P.; Williams, K. R.; Maluf, N. I.; Kovacs, G. T. A. *Sens. Actuators A* **2000**, *77*, 57-65.

(16) Kugelmass, S. M.; C., L.; DeWitt, S. H. *Proc. SPIE-Int. Soc. Opt. Eng.* **1999**, *3877*, 88-94.

(17) Kuo, T.-C.; Sloan, L. A.; Sweedler, J. V.; Bohn, P. W. *Langmuir* **2001**, *17*, 6298-6303.